1521-0103/384/1/92–101$35.00
THE JOURNAL OF PHARMACOLOGY AND EXPERIMENTAL THERAPEUTICS

dx.doi.org/10.1124/jpet.121.001095
J Pharmacol Exp Ther 384:92–101, January 2023

The Journal of PHARMACOLOGY And Experimental Therapeutics

Special Section on Non-Coding RNA: From Biomarker to Therapeutic Tool

Role of Long Non-Coding RNAs in Human-Induced Pluripotent Stem Cells Derived Megakaryocytes: A p53, HOX Antisense Intergenic RNA Myeloid 1, and miR-125b Interaction Study

Swati Dahariya, Sanjeev Raghuwanshi, Vasanth Thamodaran, Shaji R. Velayudhan, and Ravi Kumar Gutti

Stem Cell Research Laboratory, Department of Biochemistry, School of Life Sciences, University of Hyderabad, Hyderabad, India (S.D., S.R., R.K.G.) and Centre for Stem Cell Research, Christian Medical College, Vellore, India (V.T., S.R.V.)

Received July 27, 2021; accepted September 22, 2022

ABSTRACT

Megakaryocytes (MKs) are rare polyploid cells found in the bone marrow and produce platelets. Platelets are small cell fragments that are essential during wound healing and vascular hemostasis. In vitro differentiation of MKs from human-induced pluripotent stem cell–derived $CD34^+$ hematopoietic stem cells (hiPSC-HSCs) could provide an alternative treatment option for thrombocytopenic patients as a platelet source. In this approach, we developed a method to produce functional MKs from hiPSC-HSCs using a xeno-free and feeder-free condition and minimize the variation and risk from animal-derived products in cell culture. We have also investigated the genome-wide expression as well as functional significance of long noncoding RNAs (lncRNAs) in hiPSC-HSC–derived MKs to get insight into MK biology. We have performed lncRNAs expression profiling by using the Human LncProfilers qPCR Array Kit and identified 26 differentially regulated lncRNAs in hiPSC-HSC–derived MKs as compared with those in hiPSC-HSCs. HOX antisense intergenic RNA myeloid 1 (HOTAIRM1) was the most highly upregulated lncRNA in hiPSC-HSC–derived MKs and phorbol 12-myristate 13-acetate (PMA)-induced megakaryocytic-differentiating K562 cells. Furthermore, we have studied the potential mechanism of HOTAIRM1 based on the interactions between HOTAIRM1, p53, and miR-125b in PMA-induced K562 cells. Our results demonstrated that during MK maturation, HOTAIRM1 might be associated with the transcriptional regulation of p53 via acting as a decoy for miR-125b. Thus, the interaction between HOTAIRM1, p53, and miR-125b is likely involved in controlling cell cycling (cyclin D1), reactive oxygen species production, and apoptosis to support terminal maturation of MKs.

SIGNIFICANCE STATEMENT

In vitro generation of megakaryocytes (MKs) from human-induced pluripotent stem cell–derived hematopoietic stem cells (hiPSC-HSCs) could provide an alternative source of platelets for treating thrombocytopenic patients. This study has investigated the functional significance of long non-coding RNAs in hiPSC-HSC–derived MKs, which remains unclear. This study's findings suggest that the regulatory role of HOX antisense intergenic RNA myeloid 1 (HOTAIRM1) in p53-mediated regulation of cyclin D1 during megakaryocytopoiesis is to promote MK maturation by decoying miR-125b.

Introduction

Human megakaryocytes (MKs) are large, polyploid (≥8N) cells that are derived from hematopoietic stem cells. MKs are specialized precursor cells found in the bone marrow that give rise to platelets in the blood circulation (Patel et al., 2005; Richardson et al., 2005; Deutsch and Tomer, 2006; Machlus et al., 2014). The principal function of platelets in the vascular system is to prevent bleeding. Thrombocytopenia is characterized by a

This work was supported by the University of Hyderabad-Institution of Eminence Grant (No. UOH-IOE-RC3-21-006), Council of Scientific and Industrial Research [CSIR, No. 27(0343)/19/EMR-II], University Grants Commission [UGC-SAP-DRS, F.5-12/2016/DRS-I (SAP-II)], Indian Council of Medical Research (ICMR, 56/5/2019-Nano/BMS), Science and Engineering Research Board (SERB, EEQ/2018/00853), Department of Science and Technology (DST-FIST), and Department of Biotechnology (DBT, BUILDER) grants of the Government of India.
The authors declare that they have no conflict of interest.
All experiments were conducted in accord with the local regulations and laws as well as with approval from the Institutional Ethics Committee.
dx.doi.org/10.1124/jpet.121.001095.

ABBREVIATIONS: BMP4, bone morphogenetic protein 4; FACS, fluorescence-activated cell sorting; FGF2, fibroblast growth factor 2; hiPSC-HSC, human-induced pluripotent stem cell–derived hematopoietic stem cell; HOTAIRM1, HOX antisense intergenic RNA myeloid 1; IL, interleukin; lncRNA, long noncoding RNA; MK, megakaryocyte; NAC, N-Acetyl-L-cysteine; ncRNA, noncoding RNA; PE, phycoerythrin; PMA, phorbol 12-myristate 13-acetate; qRT-PCR, quantitative real-time polymerase chain reaction; ROS, reactive oxygen species; SCF, stem cell factor; TPO, thrombopoietin; VEGF-2, vascular endothelial growth factor 2; WG, Wright-Giemsa.

low platelet count ($< 1.5 \times 10^6$ cells per L) in the blood circulation. This condition can be caused by various blood disorders and factors as well as a number of medications. Human diseases related to MK development and blood platelets affect a significant portion of the population and constitute a serious health problem worldwide. Platelet transfusion is critical to maintaining normal platelet counts in patients suffering from thrombocytopenia. Ex vivo generation of MK/platelets from human-induced pluripotent stem cells could offer an alternative treatment option for patients diagnosed with thrombocytopenia and allow the study of the molecular mechanisms involved in MK development and platelet production (Liu et al., 2015; Börger et al., 2016).

A variety of cytokines and transcription factors have been implicated in megakaryocytopoieisis, but there are also new players involved in genetic regulation: non-coding RNAs (ncRNAs), such as miRNAs and long non-coding RNAs (lncRNAs). Recognizing the functional role of these molecules is an area of focus in the study of molecular regulatory mechanisms governed by different cytokines and transcription factors.

The human transcriptome consists of various RNA biotypes, including many non–protein-coding RNA transcripts that have regulatory, structural, or unidentified functions. MicroRNAs can be extensively dysregulated in multiple human diseases (Ambros, 2004; Bartel, 2004), and several miRNAs have also been implicated in the regulation of platelet biogenesis and MK development (Raghuwanshi et al., 2019a). In general, lncRNAs are characterized as ncRNAs that stretch over 200 nucleotides and lack a known protein-coding function (Saxena and Carninci, 2011). Researchers are interested in lncRNAs because their functions have been defined in several biologic processes (Tsai et al., 2010; Kaikkonen et al., 2011). Unlike miRNAs, however, the role of lncRNAs is not yet fully explored, and much less is known about the function of lncRNAs in megakaryocytopoiesis (Tian et al., 2016). Only a few studies have shown that lncRNAs play a role in cancers associated with abnormal gene expression (Ji et al., 2003; Panzitt et al., 2007; Gupta et al., 2010). Although lncRNAs have been characterized in different cells, their role in megakaryocytopoiesis has not been investigated.

Therefore, a thorough exploration of the MK transcriptome might offer an opportunity to uncover the functions of ncRNAs in the development of MKs and platelets. Hence, the purpose of this study was to standardize a protocol for the MK generation in xeno-free and defined conditions and to understand the lncRNAs profile of hiPSC-HSC–derived MKs. Furthermore, during megakaryocytic differentiation, we tried to explore the potential of the interactions between p53, HOX antisense intergenic RNA myeloid 1 (HOTAIRM1), and miR-125b.

Materials and Methods

Cell Culture. We attained hiPSC-HSCs from inStem Centre for Stem Cell Research (Vellore, India). The hiPSC-HSCs (1×10^5/mL) were cultured (5% CO_2 incubator at 37°C) serum-free in 1 mL of StemPro-34 basal media (1X) supplemented with L-glutamine (2 mM), PenStrep (1X), rhIL-6 (20 ng/mL), rhIL-3 (20 ng/mL), rhFLT3 (100 ng/mL), and rhSCF (100 ng/mL). Expansion media was changed at 2-day intervals.

On the 5th day of culture, the hiPSC-HSCs were collected and transferred to media used for differentiation of MKs: StemPro-34 basal media with L-glutamine (2 mM), PenStrep (1X), interleukin (IL)-3 (10 ng/mL), IL-11 (10 ng/mL), thrombopoietin (TPO) (50 ng/mL), vascular endothelial growth factor 2 (VEGF-2) (10 ng/mL), stem cell factor (SCF) (20 ng/mL), bone morphogenetic protein 4 (BMP4) (10 ng/mL), and fibroblast growth factor 2 (FGF2) (10 ng/mL). This optimized differentiation media offers an easy solution to generate MKs in feeder-free conditions within 5–10 days. At regular intervals (i.e., every 2 days), half of the media was substituted.

For the functional study of lncRNAs, phorbol 12-myristate 13-acetate (PMA)-induced megakaryocytic-differentiating K562 cells were used. RPMI-1640 (Invitrogen) media with 1% antibiotic antimycotic solution (Sigma) and 10% FBS was used, followed by incubation at 37°C in a 5% CO_2 incubator. K562 cells were treated with PMA (50 nM) (Sigma-Aldrich) for 72 hours to initiate megakaryocytic differentiation. After 72 hours, cells were collected to study their RNAs and proteins.

Bright-Field Imaging. On the 10th day, phase contrast micrographs (Confocal Microscope, Olympus with 405 LASER) were taken to evaluate morphologic changes on hiPSC-HSC–derived MKs.

To observe the multilobed polyploid nucleus of differentiated MKs, harvested cells were rinsed with 1X PBS and fixated on glass slides. Wright-Giemsa (WG) (Baxter) staining was performed according to the manufacturer's instructions. A confocal microscope (Zeiss LSM 510) was used to capture the images, in conjunction with the Zeiss ZEM imaging software.

Flow Cytometry Analysis. Cells (1×10^6/mL) were prepared in 1X PBS with 0.1% FBS. Cells were harvested and labeled with phycoerythrin (PE)-tagged anti-CD34 and PE–tagged anti-CD41 (BD Biosciences, and PE-tagged anti-CD61 (BD Biosciences). Ig isotype controls were used as controls for flow cytometry. All samples were analyzed for $CD34^+$, $CD41^+$, and $CD61^+$ expression using the fluorescence-activated cell sorting (FACS) Aria III flow cytometer (BD Biosciences). HiPSC-HSCs were used as a control.

Ploidy (DNA Index) Analysis. To properly calculate the DNA Index, the harvested cells were stained (1×10^6 cells per mL) using reagents from the Muse Cell Cycle Assay Kit (Merck Millipore) according to the manufacturer's instructions. The Millipore Muse Cell Cycle Assay kit comes with propidium iodide (PI) that will be detected by the Yellow detector in linear mode. PI is the most regularly used dye for quantification of DNA content, which could be assessed by employing a flow cytometer (Muse Cell Analyzer; Merck Millipore). The DNA profile of the cell culture was determined by plotting a histogram between DNA content and cell number. The experiments contained a minimum of 5000 events per run.

RNA Isolation and Quantitative RT-PCR Analysis. The miRNeasy Mini Kit (Qiagen) was used to extract the total RNA from the cell culture according to the manufacturer's instructions. Total RNA concentration was estimated using Nanodrop (Thermo Scientific), and 1 μg RNA was used as input for cDNA synthesis using EasyScript cDNA Synthesis Kit (abm) according to the manufacturer's instructions. To amplify the first strand of cDNA, specific primers were used in real-time quantitative polymerase chain reaction (qRT-PCR; Applied Biosystems) with SYBR Green FAST qPCR Master Mix (Kappa Biosystems) according to the manufacturer's instructions. The qRT-PCR was run under the following conditions: initial denaturation for 2 minutes at 52°C followed by 8 minutes at 95°C; 20 seconds at 56°C for 42 cycles; and 30 seconds at 72°C. Glyceraldehyde-3-phosphate dehydrogenase was used as the internal control to normalize the Ct values. Analysis of miR-125b expression was performed by qRT-PCR using miScript Primer Assay kit (Qiagen). Data were normalized against the internal control U6. Relative quantification was determined by the comparative ΔΔCt method ($2^{\wedge(-\Delta\Delta Ct)}$). Table 1 shows the primer sets used for the qRT-PCR.

RNA Isolation and lncRNAs Expression Profiling. For lncRNA expression profiling, the miRNeasy Mini Kit (Qiagen) was employed to extract total RNA from the cultured cells, and 1 μg of RNA was used as input for reverse transcription using the Human LncProfilers cDNA synthesis kit (System Biosciences) according to the manufacturer's instructions.

TABLE 1
Primers used in the current study

Gene/lncRNA	Primer	Sequence (5′–3′)	Amplicon Size (Nucleotides)
GAPDH	Forward	ACCACAGTCCATGCCATCAC	420
	Reverse	TCCACCACCCTGTTGCTGTA	
18S	Forward	CTCGGCAACGGATATCTCG	400–900
	Reverse	GCCCTCAACCTAATGGCTTC	
CD61	Forward	CCTGTTGGGAGTGAGGATGT	260
	Reverse	AGAGCTGCCAATAAGGCAAA	
CD41	Forward	TCAACCCTCTCAAGGTGGAC	260
	Reverse	GCAGCACAAACTGATCCAGA	
HOTAIRM1	Forward	AGGGGGTTGAAATGTGGGTG	600
	Reverse	CTTGAAAGTGGAGAAATAAAGTGCC	
TncRNA	Forward	GCTGGAGTCTTGGGCACGGC	509
	Reverse	TCAACCGAGGCCGCTGTCTC	
LUST	Forward	GCTTCAACACTGCGTGACAA	745
	Reverse	CGTGGAATCAAATGGAGTGG	
miR-125b	Forward	CTTGCCAGAAACGTCAATGGA	20
	Reverse	GTGCAACTACGTCATAGCCTG	

GAPDH, glyceraldehyde-3-phosphate dehydrogenase.

Human LncProfilers qPCR Array Kits were used for lncRNAs profiling. The differentially expressed lncRNAs between differentiated hiPSC-HSC–derived MKs and controls (iPSC-HSCs) were identified using the ΔΔCT analysis software (fold change ±2 and $P < 0.05$), available on the SBI website (https://www.systembio.com/lncrna-profiler-qpcr-array-kit-human).

Protein Extraction and Western Blot Assay. Cells were rinsed twice with 1X PBS (ice cold), followed by 30 minutes of cell lysis in radioimmunoprecipitation assay buffer (RIPA buffer) (ice cold) (Sigma) with phosphatase arrest (G-Biosciences) and protease inhibitor cocktail (Sigma) under continuous shaking at 4°C. Insoluble matter was separated and discarded from samples through centrifugation (12,000*g* at 4°C for 15 minutes). Proteins (50 μg) were separated using a 6%–12% SDS-PAGE and transferred to nitrocellulose membranes. The membranes were blocked with 5% bovine serum albumin and incubated overnight with specific primary antibodies (β-actin: Sigma; p53, Cyt C, Caspase 3, and Caspase 9: Biosciences; p21, PARP, Bcl2, BAX, and BAD: Santa Cruz). The membranes were rinsed twice with 1X Tris-buffered saline (TBS) and 1X Tris-buffered saline with 0.1% Tween 20 Detergent (TBST) buffers, followed by 1 hour of incubation with suitable peroxidase-conjugated secondary antibodies. A chemiluminescent solution, Pierce ECL Substrate (Thermo Fisher Scientific), was employed for developing protein bands on nitrocellulose membranes. For visualization, the Chemidoc Imaging System (BioRad) was used according to the manufacturer's instructions. Relative protein levels were quantified by calculating the western blot band density using ImageJ software. For normalization, β-actin was employed.

Determination of Intracellular Reactive Oxygen Species. To scavenge the ROS produced by PMA-stimulated K562 cells, the cells were treated with 5 μm N-Acetyl-L-cysteine (NAC; Sigma). To understand the effect of the intracellular ROS levels on miR-125b in the context of MK differentiation, a DCFDA assay was performed using NAC (a ROS quencher) that usually interacts with ROS to reduce intracellular ROS levels. To monitor the intracellular ROS levels, PMA-activated K562 cells (1×10^6 cells/mL) were stained with a cell permeable dye H2DCFDA (2',7'-dichlorodihydrofluorescein diacetate). Here, we measured ROS levels from different experimental timepoints such as control, 24 hours, 48 hours, and 72 hours treated with PMA (40 ng/mL). In brief, cells were rinsed with PBS and incubated with dye (10 μM) in PBS for 15 minutes in the dark at room temperature. Green fluorescence emitted by 2,7-dichlorofluorescein was quantified by a flow cytometry (BD LSR FORTESSA). Mean fluorescence intensity was graphed in scatter plots. Later, cells were harvested to analyze the miR-125b expression levels.

Cell Culture and Small Interfering RNA–HOTAIRM1 Transfection. K562 cells were cultured in RPMI-1640-GlutaMAX media (Gibco; Thermo Fisher Scientific) supplemented with 1% antibiotic-antimycotic solution (Sigma-Aldrich) and 10% FBS (Gibco; Thermo Fisher Scientific). Cells were maintained at 37°C in a 5% CO_2 humidified incubator. Cells were cultured overnight in 24-well plates (1×10^5 cells per well). To induce K562 differentiation into MKs, the culture media was supplemented with PMA (50 nM). The lncRNA HOTAIRM1-siRNAs were designed and synthesized using the Sigma-Aldrich website (sigma-aldrich.com) and transfected to PMA-induced K562 cells using the X-tremeGENE 360 Transfection Reagent (Sigma-Aldrich) and negative controls [nontargeting or nonsense small interfering RNA (siRNA) control sequence]. A defined volume of each si-HOTAIRM1 was added to the transfection samples to achieve a final concentration of 25 nM according to the manufacturer's instructions. The expression of the lncRNA HOTAIRM1 was determined via qRT-PCR to verify the occurrence of any off-target effects after three transfections with the HOTAIRM1-siRNA mixture; the aim was to successfully avoid off-target effects. Following transfection of PMA-induced K562 cells with human siRNA-HOTAIRM1 for 48 hours, cells were subjected to downstream experiments.

Statistical Analysis. All experimental studies were conducted in triplicate. Results are represented as mean ± standard deviation. The significance of variance among the groups was calculated by Student's *t* test. The biologic significance threshold and statistical significance was set at ±twofold change and $P < 0.05$, respectively. The statistical significance of the data is shown by the *P* value ($^*P < 0.05$; $^{**}P < 0.002$).

Results

MK Differentiation from iPSC-HSCs in Defined and Xeno-Free Conditions. The present study focuses on the generation of MKs from iPSC-HSCs. Previous studies have reported the differentiation of MKs from iPSC-HSCs under defined and xeno-free conditions (Liu et al., 2015; Börger et al., 2016; Hansen et al., 2018). In this culture system, we cultured iPSC-HSCs for 5 days in hematopoietic stem cell expansion media. We further transfected these cells to MK differentiation media supplemented with cytokines and growth factors (FGF2, BMP4, SCF, VEGF-2, TPO, IL-11, and IL-3), which are essential for MK differentiation and growth. At the 10th day of culture, we collected cells and analyzed them for morphologic changes. We further analyzed the expression of MK-specific markers using FACS and qRT-PCR. We analyzed polyploidy using WG staining.

After the 10th day, cell mass had increased compared with that on day 0 (Fig. 1B). About 80.3% of nonstimulated cells (day 0) expressed CD34 surface antigens specific to iPSC-HSCs

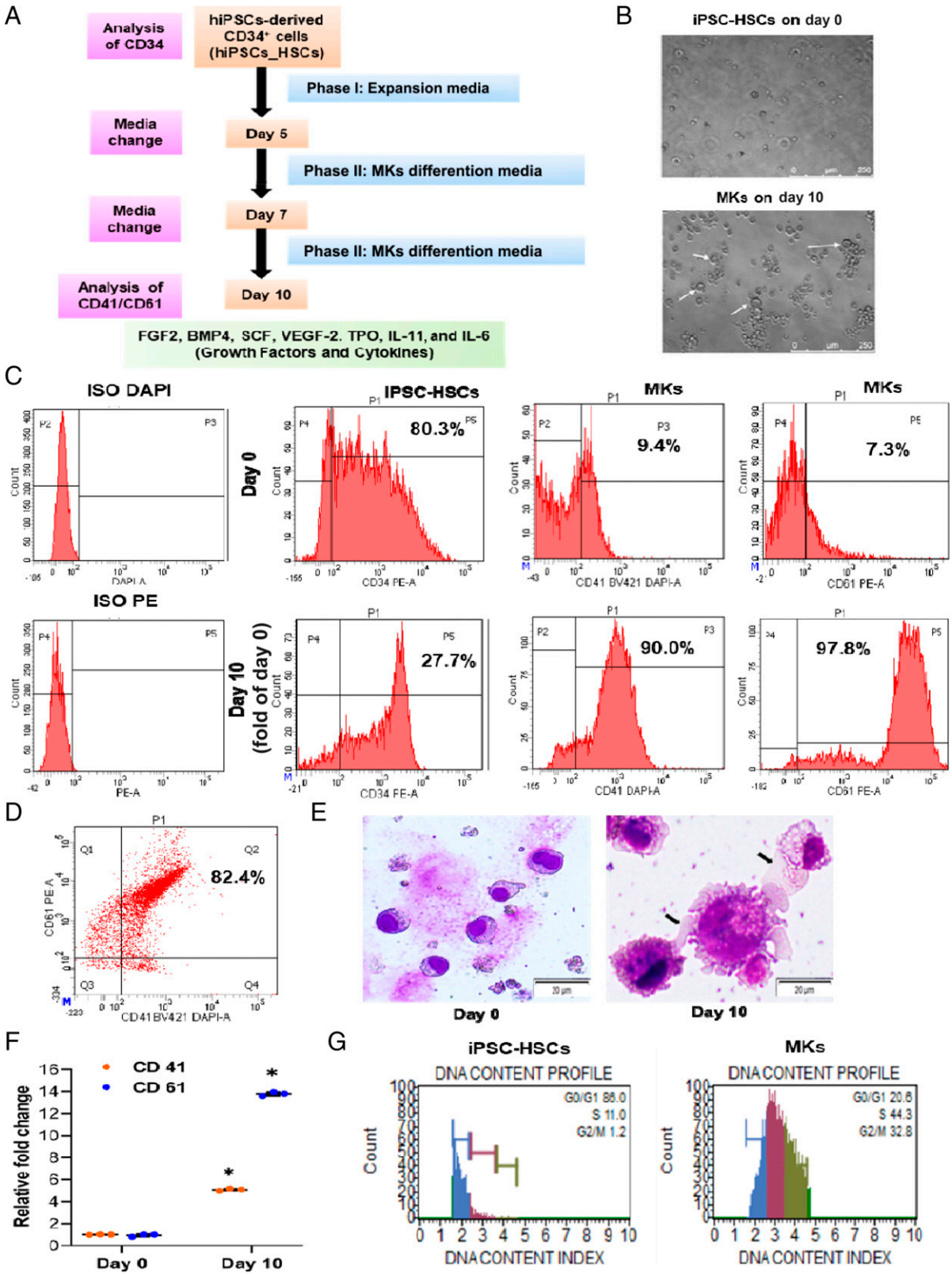

Fig. 1. Efficient differentiation of MKs from iPSC-HSCs. (A) Schematic representation of the iPSC-HSCs differentiation protocol toward MKs. (B) Phase contrast cell images on day 0 and day 10. (C) Flow cytometry histograms of the cultured suspension cells on day 0 and day 10. The suspension cells on day 0 expressed CD34 marker, and on day 10, maximum cells showed MK markers CD41 and CD61. (D) Fluorescence-activated cell sorting (FACS) analysis for double staining of MK cell surface markers (CD41/CD61) in MKs was evaluated. (E) Photomicrograph of cells stained with Giemsa showing the cell and nuclear size were increased for MKs on day 10. Scale bar, 20 μm. (F) qRT-PCR results showing fold induction of CD41 and CD61 expressions in cells of day 10 as compared with the cells of day 0 (*$P < 0.05$). (G) DNA content (polyploidy status) was increased in MKs compared with iPSC-HSCs, which was analyzed by MUSE analyzer.

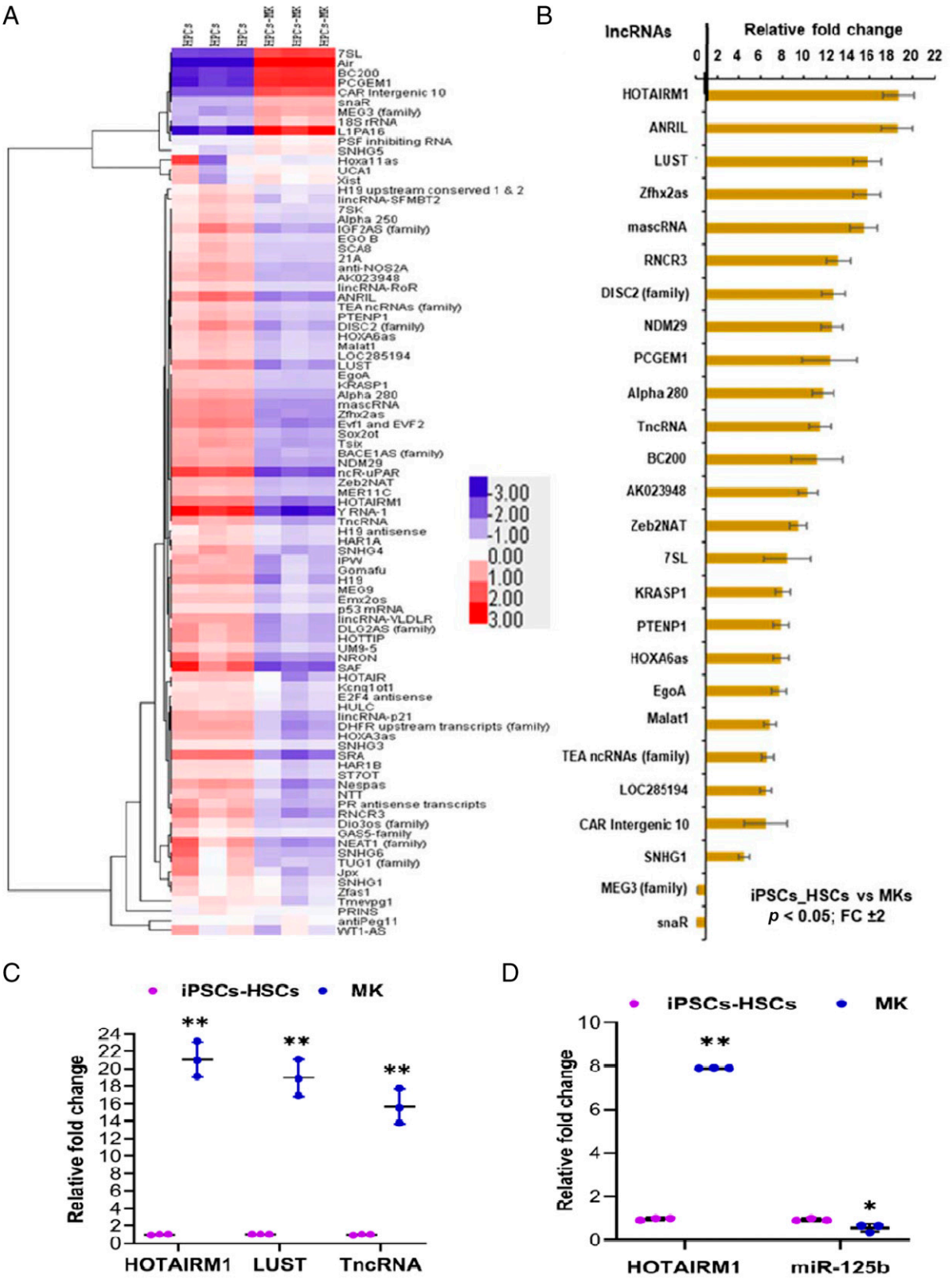

Fig. 2. LncRNA profiling and analysis of differentially expressed lncRNAs in MKs. (A) Visualization of ΔΔCt values of lncRNAs in iPSC-HSCs and MKs using heat map. (B) qRT-PCR showing top 26 (24 up- and two downregulated) most differentially expressed lncRNAs in iPSC-HSCs and MKs (*$P < 0.05$). (C) Validation of lncRNA array data through qRT-PCR analysis. The qRT-PCR reactions for HOTAIRM1, LUST, and TncRNA were repeated three times in iPSC-HSCs and MKs (**$P < 0.02$). (D) qRT-PCR results showing fold induction in the expression of HOTAIRM1 and miR-125b in iPSC-HSCs and MKs (**$P < 0.002$; *$P < 0.05$).

(Fig. 1C). Interestingly, after 10 days of culture with cytokines, >90% of the cells were MKs ($CD41^+/CD61^+$; Fig. 1, C and D) as determined using FACS. The MK surface antigens CD41 and CD61 are commonly used to define MK differentiation and maturational stages (Raghuwanshi et al., 2019b; Raghuwanshi et al., 2020). Cell morphology and nuclear size was identified in WG-stained smears of cells, and the results were compared between day 0 and day 10. In this study, after the 10th day, we have observed MKs with large sizes having polyploid multilobed nucleus (Fig. 1E). However, when measuring the ploidy of the MKs, DNA content is presented as DNA Index, which is the ratio of DNA content of the experimental sample to the corresponding control (normal diploid) population. In general, cells in G0 or G1 phases contain normal diploid chromosomal content (2n DNA), whereas cells in G2, and just prior to mitosis, consist of double DNA (4n) content as compared to the normal quantity. This analysis was performed to determine the content of DNA in the range of 2n, 4n, and so on, as DNA synthesis occurs in S phase. Hence, we have focused our interest to diploid cells that produce polyploid progeny since this is a distinctive feature of MKs. Increased ploidy levels as evaluated by cell cycle analysis was detected in hiPSC-HSC–derived MKs as compared with hiPSC-HSCs on the 10th day (Fig. 1G).

Differential Expression Analysis of lncRNAs in iPSC-HSCs Versus MKs. Following the confirmation of the MK differentiation from hiPSC-HSCs, we have identified the expression profile of lncRNAs in control (hiPSC-HSCs) and experiment (MKs) groups using Human LncProfilers qPCR Array (SBI). The differential expression of lncRNAs between hiPSC-HSCs and MKs was analyzed via ΔΔCt analysis software (https://www.systembio.com/lncrna-profiler-qpcr-array-kit-human). Figure 2A shows a heat map with the Ct values of 90 lncRNAs, which were profiled in hiPSC-HSCs and MKs groups. Of the 90 lncRNAs analyzed in MKs, only 26 (28.88%) lncRNAs showed statistically significant difference with respect to hiPSC-HSCs ($P < 0.05$; fold change ±2.0; Fig. 2B). Of these 26 differentially regulated lncRNAs, 24 (26.66%) genes were upregulated, whereas only two (2.22%) genes were downregulated (Fig. 2B). HOTAIRM1 lncRNA was identified as the highest upregulated in MKs in comparison with hiPSC-HSCs. Furthermore, by using lncRNA-specific primers through qRT-PCR, Array-Based Gene Expression Profile was validated. To confirm these significant lncRNAs signature performance in MKs, we validated the expression of randomly selected top three lncRNAs (HOTAIRM1, LUST, and TncRNA) out of 24 upregulated lncRNAs by qRT-PCR. We quantified expression of the highest-upregulated lncRNAs, HOTAIRM1, LUST, and TncRNA, and similar distinctions between hiPSC-HSCs and MKs were observed in qRT-PCR result ($P < 0.02$; Fig. 2C). In both experiments, a more than twofold difference in the expression levels of lncRNAs was observed. These results support the use of qPCR array as a screening tool and emphasize the need for the validation of the array results.

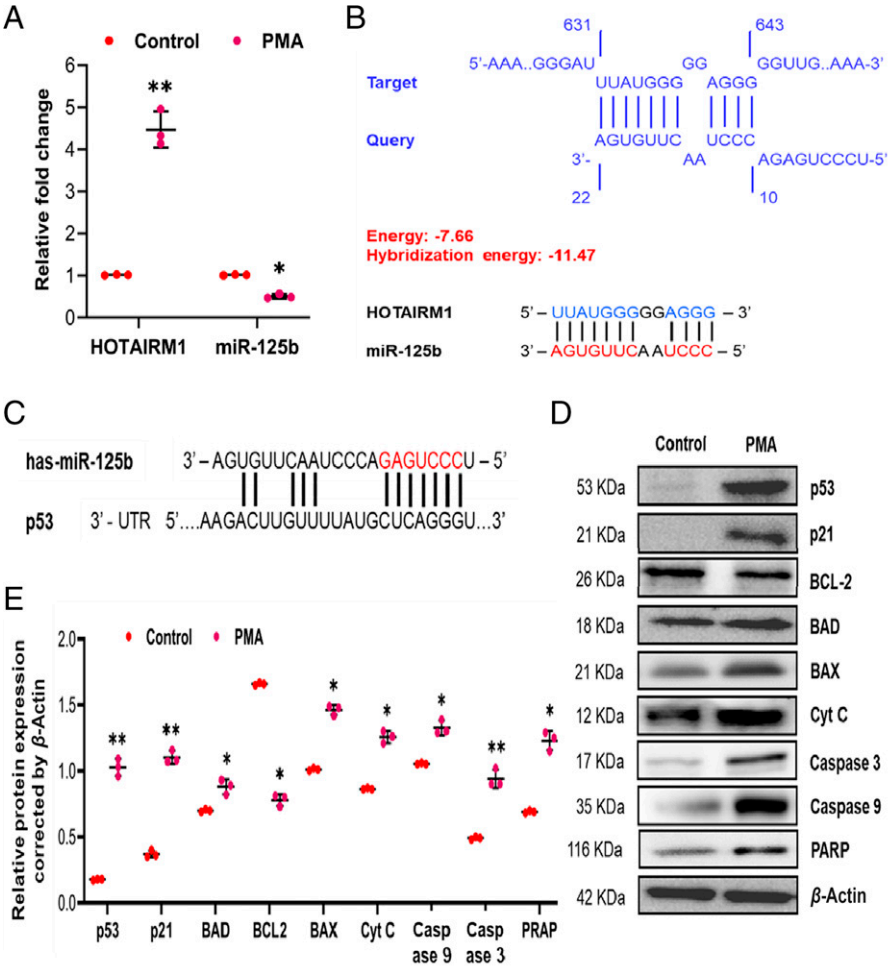

Fig. 3. p53, HOTAIRM1, and miR-125b interaction study in PMA-induced megakaryocytic-differentiating cell line model. (A) qRT-PCR results show the differential expression of HOTAIRM1 and miR-125b in PMA-induced MKs in comparison with control (uninduced) K562 cells (**$P < 0.002$). (B) HOTAIRM1 and miR-125b sequence interaction. Minimum free energy duplex of miR-125b and HOTAIRM1 was determined by using IntaRNA tool. (C) RNAhybrid prediction analysis of miR-125b with its target gene p53 by using TargetScan tool. (D) The protein levels of p53, p21, and components of intrinsic apoptosis pathway were increased in PMA-induced MKs in comparison with control (**$P < 0.02$). (E) Quantification of protein expression with respect to β-actin (**$P < 0.02$; *$P < 0.01$).

HOTAIRM1, a Natural Sponge, Likely to Be Associated with the p53 mRNA Regulation and Protein Expression by Competing with miR-125b during Megakaryocytic Differentiation. In this study, we used a well defined PMA-induced megakaryocytic differentiation of a K562 cell line model to explore the HOTAIRM1-regulated mechanism in MKs. Interestingly, validation results confirmed that HOTAIRM1 expression was significantly increased (~20-fold; $P < 0.002$; Fig. 2C) in hiPSC-HSC–derived MKs as compared with control iPSC-HSCs. In addition, we observed that the expression pattern of HOTAIRM1 in PMA-induced megakaryocytic K562 cells was closely related with its expression in iPSC-HSC–derived MKs (~4.7-fold; $P < 0.002$; Fig. 3A). In the present study, it was observed that during the megakaryocytic differentiation initiation using PMA in K562 cell line, p53 protein levels were significantly increased (~sevenfold; $^{**}P < 0.02$, $^{*}P < 0.01$ Fig. 3, D and E). It has been demonstrated that the lncRNA HOTAIRM1 serves as a decoy for miR-125b as well as for other miRNAs, keeping them away from p53 mRNAs (Ng et al., 2019). We have also found significant interactions between lncRNA HOTAIRM1 and miR-125b (Fig. 3B) by employing IntaRNA tool (http://rna.informatik.uni-freiburg.de/IntaRNA). miR-125b is a well known oncomiR that negatively regulates p53 (Le et al., 2009; Shaham et al., 2012). We have also found that the potential target gene of miR-125b is p53 (Fig. 3C) by using TargetScan Human (http://www.targetscan.org/vert_72/). Furthermore, it was observed that miR-125b expression level was significantly lower in both iPSC-HSC–derived MKs and PMA-induced MKs in comparison with control groups (iPSC-HSCs and untreated K562 cells) ($P < 0.002$; Figs. 2D and 3A).

HOTAIRM1 Upregulates p53 Expression and Is Involved in MK Maturation via Regulating Downstream Target Genes P21 and Cyclin D1, Apoptosis Regulators, and ROS. To understand the functional role of p53 in MKs, expression levels of three known transcriptional targets of p53 (p21, BAD, and Bcl-2) were studied. In the present study, p21 and BAD were upregulated, and Bcl-2 was downregulated in protein expression analysis by western blotting in PMA-induced MKs in comparison with control ($^{**}P < 0.02$, $^{*}P < 0.01$; Fig. 3, D and E). Furthermore, we have also observed the increased production of ROS by flow cytometry and MK-specific late marker CD61 expression by qRT-PCR at different timepoints during megakaryocytic maturation ($^{**}P < 0.02$; Fig. 4, A and B). It was observed that p53, p21, BAX, and BAD were upregulated in PMA-induced megakaryocytic cells ($^{**}P < 0.02$, $^{*}P < 0.01$; Fig. 3, D and E). In contrast, Bcl-2 expression was downregulated, and it is known to be negatively affected by p53 ($^{**}P < 0.02$, $^{*}P < 0.01$; Fig. 3, D and E) (Ravid et al., 2002). Our results also demonstrated the activation of PARP cleavage and of caspase cascade known for markers for the components of classic intrinsic apoptosis pathway during terminal maturation of MKs ($^{**}P < 0.02$, $^{*}P < 0.01$; Fig. 3, D and E) (Josefsson et al., 2011; Kile, 2014; McArthur et al., 2018; Kovuru et al., 2020).

To further understand whether ROS generation is important for megakaryocyte maturation, we performed PMA-induced cell differentiation experiments employing NAC (an ROS quencher). NAC associates directly with ROS to function as a scavenger of oxygen free radicals, thereby intracellularly reducing the ROS levels. During differentiation experiments, PMA-induced cells showed

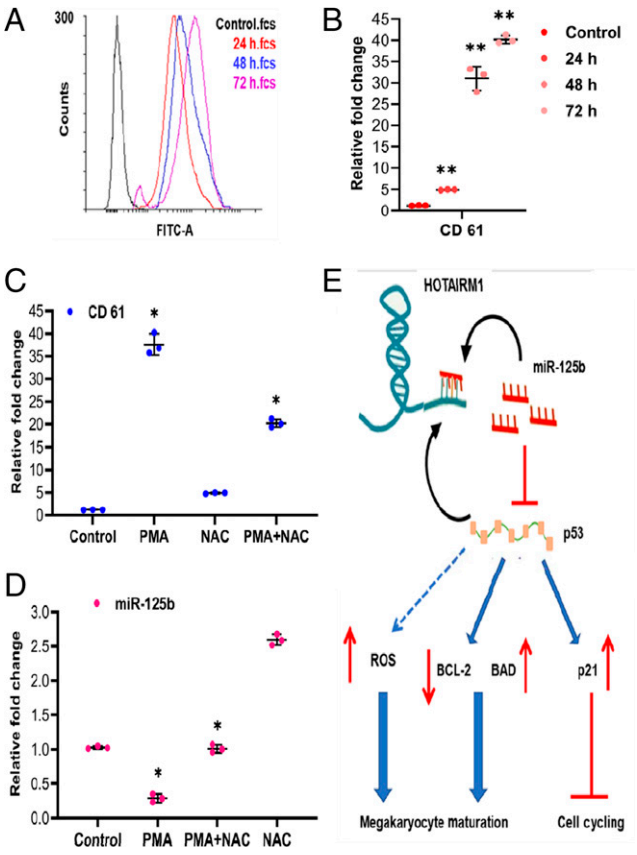

Fig. 4. PMA-induced MK differentiation involves ROS production during maturation. (A) For measurement of intracellular ROS production in cells, the 2',7'-dichlorofluorescin diacetate (DCFH-DA) assay was performed and analyzed by flow cytometry. (B) qRT-PCR analysis shows the increased expression of MK marker CD61 during PMA-induced MK maturation of K562 ($^{**}P < 0.02$). (C) In qRT-PCR analysis, MK marker CD61 expression was increased in PMA-treated cells in comparison with control, whereas it decreased in NAC-treated cells ($^{**}P < 0.05$). (D) miR-125b expression was higher in ROS scavenger NAC-treated cells compared with untreated controls but lower in PMA-treated cells ($^{**}P < 0.05$). (E) The pictorial representation of the crosstalk between lncRNA (HOTAIRM1), miRNA (miR-125b), and p53 during MK development.

that ROS downregulates miR-125b expression in matured MKs, which shows higher megakaryocytic marker CD61 expression in comparison with control ($P < 0.05$; Fig. 4, C and D). Cells treated with NAC showed no significant change in CD61 marker expression in comparison with control ($P < 0.05$; Fig. 4C). However, upon addition of PMA and NAC together, cells showed elevated levels of CD61 expression compared with NAC-treated cells ($P < 0.05$; Fig. 4C); however, the expression was lower as compared with PMA-induced cells. Taken together, this data supports the notion that ROS production is required for megakaryocyte maturation, which is associated with the p53 expression depending on the miR-125b status ($P < 0.05$; Fig. 4, C and D).

Suppression of lncRNA HOTAIRM1 Expression Induces Impairment in the Differentiation and Maturation of PMA-Induced K562 Cells. To determine the function of lncRNA HOTAIRM1 in MK differentiation and maturation, we used siRNA-HOTAIRM1 to downregulate the lncRNA HOTAIRM1 expression and detected its effects on cell cycle regulators (p53, p21, and cyclin D1) and MK-specific cell surface markers, including miR-125b expression. After 48 hours of

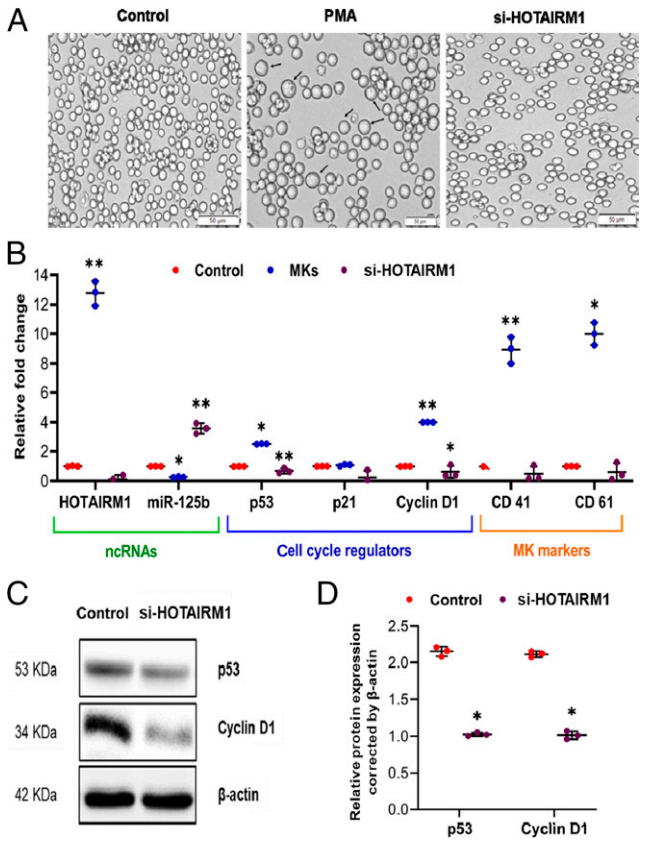

Fig. 5. Suppression of lncRNA HOTAIRM1 expression induce the impairment of differentiation and maturation of PMA-induced K562 cells. (A) si-HOTAIRM1–transfected cells show similar morphology to control as compared with PMA-induced megakaryocytic cells. Magnification, 20×; scale bar, 50 μm. (B) qRT-PCR results show that si-HOTAIRM1 transfection elevated the level of miR-125b, which further reduced the expression of its respective target genes (**$P < 0.02$; *$P < 0.01$). (C) si-HOTAIRM1 transfection significantly inhibits the protein expression of p53 and cyclin D1 as analyzed by western blot. (D) A plot showing the actual mean band intensity of the blots (*$P < 0.01$).

transfection, cells were collected and observed under a bright-field microscope. For both the control group and the group transfected with siRNA-HOTAIRM1, no large-sized cells like MKs were observed (Fig. 5A). Next, we investigated gene expression for cyclin D1, p53, and p21 by qRT-PCR analysis. This revealed that inhibition of lncRNA HOTAIRM1 expression in siRNA-transfected PMA-induced K562 cells could not generate cyclin D1, p53, and p21 respective mRNAs, and as a result, their protein levels were decreased considerably (**$P < 0.02$, *$P < 0.01$; Fig. 5, B–D). Furthermore, significant upregulation of miR-125b level was observed in the si-HOTAIRM1–treated PMA-induced megakaryocytic K562 cells in comparison with control (**$P < 0.02$, *$P < 0.01$; Fig. 5B). To determine the lncRNA HOTAIRM1 role in MK maturation, the impact of HOTAIRM1 downregulation on MK-specific cell surface markers (CD41 and CD61) was studied. RT-PCR results demonstrated that CD41 and CD61 expressions were considerably decreased in the si-HOTAIRM1–treated group (**$P < 0.02$, *$P < 0.01$; Fig. 5B). Therefore, these results might imply that downregulation of lncRNA HOTAIRM1 expression might affect MK differentiation and maturation by influencing the expression of miR-125b, which might have an impact on p53 and p21 expression to stimulate MK maturation.

TABLE 2
Concentration of growth factors used for MK differentiation

Sl. No.	Growth Factors	Stock Conc. (μg/mL)	Working Conc. (ng/mL)
1	FGF2	10	10
2	BMP4	50	10
3	SCF	100	20 (2.0 μL/3 mL)
4	VEGF-2	50	10
5	TPO	50	50 (3.0 μL/3 mL)
6	IL-11	2	10 (15.0 μL/3 mL)
7	IL-6	10	10(3.0 μL/3 mL)

Discussion

In the present study, we differentiated MKs from iPSC-HSCs under defined and xeno-free conditions. For efficient production of MKs, we modified culture conditions such as culture media composition (Fig. 1A; Table 2) from previously reported protocols (Liu et al., 2015; Börger et al., 2016; Hansen et al., 2018). In contrast to previous studies, the present work uses the same media composition throughout the MK differentiation phase. In addition, the MK differentiation had been achieved on day 11 (Hansen et al., 2018) and day 19 (Liu et al., 2015; Börger et al., 2016), whereas we report the MK differentiation on day 10, which was attributed to the modifications made to the media composition.

The polyploidization is the crucial event of megakaryocytopoiesis, and the large, polyploid-multilobed nucleus is considered as the hallmark of matured MKs (Odell et al., 1970). Also, the expression of MK-specific markers (CD41/CD61) was further confirmed by quantifying their mRNA levels using qRT-PCR. We observed a steadily increasing expression of both the CD41 (∼sixfold) and CD61 (∼15 fold) MK-marker mRNAs after the 10th day of the treatment with cytokines in comparison with day 0 ($P < 0.05$; Fig. 1F). We developed a proficient differentiation system for MK generation from hiPSC-HSCs under feeder-free and serum-free conditions. These results indicate the feasibility to generate MKs from hiPSC-HSCs. We used a defined and basic differentiation system to generate MKs from hiPSC-HSCs and further studied their role in the molecular regulation of megakaryocytopoiesis.

After achieving MK differentiation from hiPSC-HSCs, we studied the lncRNAs expression profile in both the experiment (MKs) and control (hiPSC-HSCs) groups, thereby defining the role of lncRNAs during MK differentiation. Most recent studies have shown the functional significance of different lncRNAs in the regulation of major biologic processes, such as cancer development and progression, chromatin remodeling, and cell pluripotency (Dinger et al., 2008; Gupta et al., 2010; Mizutani et al., 2012; Klattenhoff et al., 2013; Fang et al., 2014). Although a fair number of lncRNAs have been recognized in different lncRNA-profiling studies, only a few have been experimentally validated in human hematopoiesis (Garzon et al., 2014). Recent studies indicate that HOTAIRM1 is involved in myeloid differentiation. However, the underlying mechanism of HOTAIRM1-mediated regulation in megakaryocytic maturation has not been determined.

Induction of MK differentiation in K562 cells using PMA is a classic and well understood model to study megakaryocytic differentiation. However, this progression is accompanied by cell morphologic changes, increased MK-specific marker expression, cell growth arrest, etc. (Huang et al., 2014; Raghuwanshi et al., 2020). Interestingly, HOTAIRM1 was significantly

upregulated in both model systems. Under ordinary circumstances, the expression of HOTAIRM1 is constrained only to the myeloid lineage, and it is associated with myeloid cell differentiation (Zhang et al., 2009). In addition, recent literature has shown the regulatory interactions among p53 and HOTAIRM1 (Jain et al., 2016; Jain and Barton, 2018). p53-dependent alterations in chromatin state regulate the lncRNA HOTAIRM1 during the human embryonic stem cell differentiation. The lncRNA HOTAIRM1 is induced by p53 only when human embryonic stem cells were differentiated toward definitive ectoderm and mesoderm, but not endoderm, lineages (Jain et al., 2016). The expression of miR-125b is increased in acute megakaryocytic leukemia associated with Down syndrome (Shaham et al., 2012). A possible explanation may be that the potential role of p53-dependent expression of differentiation-specific lncRNA HOTAIRM1 can be able to protect p53 mRNA from miR-125b–mediated translation during MK maturation (Fig. 4E).

p21 has been extensively studied in MKs, and the expression of p53 and p21 is increased during MK maturation (Ravid et al., 2002; Fuhrken et al., 2008). BAD and BAX belong to the Bcl-2 family as proapoptotic proteins, which inhibit the antiapoptotic function of Bcl-2 (Jiang et al., 2007). Members of the Bcl-2 family are directly associated with MK maturation and apoptosis (Avanzi et al., 2015; Kovuru et al., 2020).

In the context of megakaryocytopoiesis, ROS levels are elevated during megakaryocytic differentiation and maturation (Chen et al., 2013; Raghuwanshi et al., 2020). Furthermore, ROS production was associated with p53 expression, which depended on miR-125b expression status (Macip et al., 2003). ROS are crucial for MK differentiation and overall development (Chen et al., 2013), as well as for the complete megakaryocytopoiesis process. Therefore, the 2,7-dichloro-dihydro-fluorescein-diacetate assay was performed to measure ROS levels at different days of MK differentiation. A continuous induction of ROS levels during the MK differentiation process was clearly evident from our results (Fig. 4A).

Our results are consistent with previous reports, which identified the functional role of p53 in the regulation of endomitosis and polyploidization by decelerating cell cycling and promoting apoptosis to initiate terminal maturation of MKs (Fuhrken et al., 2008). PMA activates NADPH oxidase and increases ROS production. ROS are involved directly or indirectly in every step of the epigenetic alterations of miRNAs and p53 gene expression (Kuwabara et al., 2015). Furthermore, existing literature highlights a reciprocal association between microRNA pathway and ROS signaling that results in diverse biologic effects in differentiating cells. In the context of MK differentiation and development, increased levels of ROS were found to suppress miR-125 expression and induce p53 expression in MKs to regulate megakaryopoiesis. Thus, we report that the interactions among HOTAIRM1, p53, and miR-125b could be associated with cell cycle regulation, ROS production, and activation of intrinsic apoptosis during megakaryocytopoiesis (Fig. 4E).

These data suggest that transfection of PMA-induced megakaryocytic K562 cells with HOTAIRM1-siRNA results in increased miR-125 expression. This is due to a decrease in the expression of its putative target, p53, as well as downstream targets. Alternatively, in both the control group and the group transfected with si-HOTAIRM1, no visual changes were observed. Next, the expressions of MK-specific markers were not significantly altered after the si-HOTAIRM1 transfection in PMA-induced megakaryocytic K562 cells, which verified the absence or differentiation of MK-like cells. These findings suggest that the HOTAIRM1 lncRNA may promote p53 gene expression by decoying miR-125b, thereby influencing differentiation and maturation of MKs. Thus, our findings revealed the functional role of HOTAIRM1 lncRNA in p53-mediated regulation of cyclin D1 as well as ROS production: to trigger the intrinsic apoptosis pathway during megakaryocytopoiesis by decoying miR-125b (Fig. 4E).

Conclusion

In the present work, we report a differential lncRNAs expression profile in MKs derived from hiPSC-HSCs. This will provide the foundation for future studies of the biologic functions of lncRNAs in the development of MKs. We found that most of the differentially expressed lncRNAs were upregulated in MKs compared with those in hiPSC-HSCs. Furthermore, to confirm these significant lncRNA signature performances, we validated the expression of three lncRNAs (HOTAIRM1, LUST, and TncRNA), out of 24 upregulated lncRNAs, by qRT-PCR. We observed similar distinctions between hiPSC-HSCs and MKs. LncRNAs play a vital role in the regulation of gene expression during development as well as differentiation. The upregulated lncRNAs identified may have functional roles in gene regulation during MK differentiation/maturation. Specifically, HOTAIRM1 was identified and confirmed as the highly upregulated lncRNA in hiPSC-HSC–derived MKs. In addition to interacting with proteins as a scaffold, the lncRNA HOTAIRM1 could exert its functional effects on several gene expressions by acting as a miRNA sponge/decoy for a number of miRNAs. We also found that the treatment of K562 cells with PMA induces HOTAIRM1 expression, similar to hiPSC-HSC–derived MKs. Moreover, we noticed that p53-dependent HOTAIRM1, unlike miR-125b, a positive regulator of p53, was significantly upregulated in PMA-induced MKs. Importantly, we demonstrated that during MK maturation, the lncRNA HOTAIRM1 might be associated with the transcriptional regulation of p53, which in turn could act as a decoy for miR-125b, keeping them away from p53 mRNA. In downstream steps, p53 can also regulate the expression of apoptotic genes and promote ROS production, which is essential during megakaryocytopoiesis, by regulating miRNAs expression. Thus, p53, along with HOTAIRM1, via regulating p21, components of BAK/Bax pathway expression, and ROS production, enhances maturation and apoptosis in MK development. However, further experiments are necessary to validate the associations between HOTAIRM1, p53, and miR-125b, as well as the functional effects of these associations in MK development.

Acknowledgments

Dahariya S, Raghuwanshi S, and Gutti R thank School of Life Sciences, University of Hyderabad for providing the research facilities required to perform the work. The authors would like to thank Editage (www.editage.com) for English language editing. The authors also thank CSIR-UGC for the fellowship.

Authorship Contributions

Participated in research design: Dahariya, Gutti.
Conducted experiments: Dahariya.

Performed data analysis: Dahariya, Raghuwanshi, Thamodaran, Velayudhan, Gutti.

Wrote or contributed to the writing of the manuscript: Dahariya, Raghuwanshi, Gutti.

References

Ambros V (2004) The functions of animal microRNAs. *Nature* **431**:350–355.

Avanzi MP, Izak M, Oluwadara OE, and Mitchell WB (2015) Actin inhibition increases megakaryocyte proplatelet formation through an apoptosis-dependent mechanism. *PLoS One* **10**:e0125057.

Bartel DP (2004) MicroRNAs: genomics, biogenesis, mechanism, and function. *Cell* **116**:281–297.

Börger AK, Eicke D, Wolf C, Gras C, Aufderbeck S, Schulze K, Engels L, Eiz-Vesper B, Schambach A, Guzman CA, et al. (2016) Generation of hla-universal ipsc-derived megakaryocytes and platelets for survival under refractoriness conditions. *Mol Med* **22**:274–285.

Chen S, Su Y, and Wang J (2013) ROS-mediated platelet generation: a microenvironment-dependent manner for megakaryocyte proliferation, differentiation, and maturation. *Cell Death Dis* **4**:e722.

Deutsch VR and Tomer A (2006) Megakaryocyte development and platelet production. *Br J Haematol* **134**:453–466.

Dinger ME, Amaral PP, Mercer TR, Pang KC, Bruce SJ, Gardiner BB, Askarian-Amiri ME, Ru K, Soldà G, Simons C, et al. (2008) Long noncoding RNAs in mouse embryonic stem cell pluripotency and differentiation. *Genome Res* **18**:1433–1445.

Fang K, Han BW, Chen ZH, Lin KY, Zeng CW, Li XJ, Li JH, Luo XQ, and Chen YQ (2014) A distinct set of long non-coding RNAs in childhood MLL-rearranged acute lymphoblastic leukemia: biology and epigenetic target. *Hum Mol Genet* **23**:3278–3288.

Fuhrken PG, Apostolidis PA, Lindsey S, Miller WM, and Papoutsakis ET (2008) Tumor suppressor protein p53 regulates megakaryocytic polyploidization and apoptosis. *J Biol Chem* **283**:15589–15600.

Garzon R, Volinia S, Papaioannou D, Nicolet D, Kohlschmidt J, Yan PS, Mrózek K, Bucci D, Carroll AJ, Baer MR, et al. (2014) Expression and prognostic impact of lncRNAs in acute myeloid leukemia. *Proc Natl Acad Sci USA* **111**:18679–18684.

Gupta RA, Shah N, Wang KC, Kim J, Horlings HM, Wong DJ, Tsai MC, Hung T, Argani P, Rinn JL, et al. (2010) Long non-coding RNA HOTAIR reprograms chromatin state to promote cancer metastasis. *Nature* **464**:1071–1076.

Hansen M, Varga E, Aarts C, Wust T, Kuijpers T, von Lindern M, and van den Akker E (2018) Efficient production of erythroid, megakaryocytic and myeloid cells, using single cell-derived iPSC colony differentiation. *Stem Cell Res (Amst)* **29**:232–244.

Huang R, Zhao L, Chen H, Yin RH, Li CY, Zhan YQ, Zhang JH, Ge CH, Yu M, and Yang XM (2014) Megakaryocytic differentiation of K562 cells induced by PMA reduced the activity of respiratory chain complex IV. *PLoS One* **9**:e96246.

Jain AK and Barton MC (2018) p53: emerging roles in stem cells, development and beyond. *Development* **145**:dev158360.

Jain AK, Xi Y, McCarthy R, Allton K, Akdemir KC, Patel LR, Aronow B, Lin C, Li W, Yang L, et al. (2016) LncPRESS1 Is a p53-Regulated LncRNA that Safeguards Pluripotency by Disrupting SIRT6-Mediated De-acetylation of Histone H3K56. *Mol Cell* **64**:967–981.

Ji P, Diederichs S, Wang W, Böing S, Metzger R, Schneider PM, Tidow N, Brandt B, Buerger H, Bulk E, et al. (2003) MALAT-1, a novel noncoding RNA, and thymosin β4 predict metastasis and survival in early-stage non-small cell lung cancer. *Oncogene* **22**:8031–8041.

Jiang P, Du W, and Wu M (2007) p53 and Bad: remote strangers become close friends. *Cell Res* **17**:283–285.

Josefsson EC, James C, Henley KJ, Debrincat MA, Rogers KL, Dowling MR, White MJ, Kruse EA, Lane RM, Ellis S, et al. (2011) Megakaryocytes possess a functional intrinsic apoptosis pathway that must be restrained to survive and produce platelets. *J Exp Med* **208**:2017–2031.

Kaikkonen MU, Lam MTY, and Glass CK (2011) Non-coding RNAs as regulators of gene expression and epigenetics. *Cardiovasc Res* **90**:430–440.

Kile BT (2014) The role of apoptosis in megakaryocytes and platelets. *Br J Haematol* **165**:217–226.

Klattenhoff CA, Scheuermann JC, Surface LE, Bradley RK, Fields PA, Steinhauser ML, Ding H, Butty VL, Torrey L, Haas S, et al. (2013) Braveheart, a long noncoding RNA required for cardiovascular lineage commitment. *Cell* **152**:570–583.

Kovuru N, Raghuwanshi S, Sharma DS, Dahariya S, Pallepati A, and Gutti RK (2020) Endoplasmic reticulum stress induced apoptosis and caspase activation is mediated through mitochondria during megakaryocyte differentiation. *Mitochondrion* **50**:115–120.

Kuwabara WMT, Zhang L, Schuiki I, Curi R, Volchuk A, and Alba-Loureiro TC (2015) NADPH oxidase-dependent production of reactive oxygen species induces endoplasmatic reticulum stress in neutrophil-like HL60 cells. *PLoS One* **10**:e0116410.

Le MTN, Teh C, Shyh-Chang N, Xie H, Zhou B, Korzh V, Lodish HF, and Lim B (2009) MicroRNA-125b is a novel negative regulator of p53. *Genes Dev* **23**:862–876.

Liu Y, Wang Y, Gao Y, Forbes JA, Qayyum R, Becker L, Cheng L, and Wang ZZ (2015) Efficient generation of megakaryocytes from human induced pluripotent stem cells using food and drug administration-approved pharmacological reagents. *Stem Cells Transl Med* **4**:309–319.

Machlus KR, Thon JN, and Italiano Jr JE (2014) Interpreting the developmental dance of the megakaryocyte: a review of the cellular and molecular processes mediating platelet formation. *Br J Haematol* **165**:227–236.

Macip S, Igarashi M, Berggren P, Yu J, Lee SW, and Aaronson SA (2003) Influence of induced reactive oxygen species in p53-mediated cell fate decisions. *Mol Cell Biol* **23**:8576–8585.

McArthur K, Chappaz S, and Kile BT (2018) Apoptosis in megakaryocytes and platelets: the life and death of a lineage. *Blood* **131**:605–610.

Mizutani R, Wakamatsu A, Tanaka N, Yoshida H, Tochigi N, Suzuki Y, Oonishi T, Tani H, Tano K, Ijiri K, et al. (2012) Identification and characterization of novel genotoxic stress-inducible nuclear long noncoding RNAs in mammalian cells. *PLoS One* **7**:e34949.

Ng M, Heckl D, and Klusmann JH (2019) The Regulatory Roles of Long Noncoding RNAs in Acute Myeloid Leukemia. *Front Oncol* **9**:570.

Odell Jr TT, Jackson CW, and Friday TJ (1970) Megakaryocytopoiesis in rats with special reference to polyploidy. *Blood* **35**:775–782.

Panzitt K, Tschernatsch MMO, Guelly C, Moustafa T, Stradner M, Strohmaier HM, Buck CR, Denk H, Schroeder R, Trauner M, et al. (2007) Characterization of HULC, a novel gene with striking up-regulation in hepatocellular carcinoma, as noncoding RNA. *Gastroenterology* **132**:330–342.

Patel SR, Hartwig JH, and Italiano Jr JE (2005) The biogenesis of platelets from megakaryocyte proplatelets. *J Clin Invest* **115**:3348–3354.

Raghuwanshi S, Dahariya S, Musvi SS, Gutti U, Kandi R, Undi RB, Sahu I, Gautam DK, Paddibhatla I, and Gutti RK (2019a) MicroRNA function in megakaryocytes. *Platelets* **30**:809–816.

Raghuwanshi S, Dahariya S, Sharma DS, Kovuru N, Sahu I, and Gutti RK (2020) RUNX1 and TGF-β signaling cross talk regulates Ca^{2+} ion channels expression and activity during megakaryocyte development. *FEBS J* **287**:5411–5438.

Raghuwanshi S, Sharma DS, Kandi R, Kovuru N, Dahariya S, Musvi SS, Venkatakrishnan AC, Pallepati A, and Gutti RK (2019b) Pituitary adenylate cyclase-activating polypeptide (PACAP): Differential effects on neonatal vs adult megakaryocytopoiesis. *Thromb Res* **175**:59–60.

Ravid K, Lu J, Zimmet JM, and Jones MR (2002) Roads to polyploidy: the megakaryocyte example. *J Cell Physiol* **190**:7–20.

Richardson JL, Shivdasani RA, Boers C, Hartwig JH, and Italiano Jr JE (2005) Mechanisms of organelle transport and capture along proplatelets during platelet production. *Blood* **106**:4066–4075.

Saxena A and Carninci P (2011) Long non-coding RNA modifies chromatin: epigenetic silencing by long non-coding RNAs. *BioEssays* **33**:830–839.

Shaham L, Binder V, Gefen N, Borkhardt A, and Izraeli S (2012) MiR-125 in normal and malignant hematopoiesis. *Leukemia* **26**:2011–2018.

Tian X, Tian J, Tang X, Ma J, and Wang S (2016) Long non-coding RNAs in the regulation of myeloid cells. *J Hematol Oncol* **9**:99.

Tsai M, Manor O, Wan Y, Mosammaparast N, Wang JK, Lan F, Shi Y, Segal E, and Chang HY (2010) Long Noncoding RNA as Modular Scaffold of Histone Modification Complexes. *Science* **329**:689–693.

Zhang X, Lian Z, Padden C, Gerstein MB, Rozowsky J, Snyder M, Gingeras TR, Kapranov P, Weissman SM, and Newburger PE (2009) A myelopoiesis-associated regulatory intergenic noncoding RNA transcript within the human HOXA cluster. *Blood* **113**:2526–2534.

Address correspondence to: Ravi Kumar Gutti, Ph.D., Department of Biochemistry, School of Life Sciences, University of Hyderabad, Hyderabad 500046, India. E-mail: guttiravi@gmail.com